Catena 139 (2016) 199–213

Contents lists available at ScienceDirect

Catena

journal homepage: www.elsevier.com/locate/catena

A channel evolution model for subtropical macrochannel systems

C.J. Thompson [a,*], J. Croke [a,b], K. Fryirs [c], J.R. Grove [d]

[a] School of Geography Planning and Environmental Management, University of Queensland, Qld, Australia
[b] DSITI, Queensland Government, Qld, Australia
[c] Department of Environmental Sciences, Macquarie University, North Ryde, NSW, Australia
[d] School of Geography, University of Melbourne, Vic, Australia

ARTICLE INFO

Article history:
Received 9 June 2015
Received in revised form 17 December 2015
Accepted 21 December 2015
Available online xxxx

Keywords:
Channel evolution model
Cycle of erosion
Incision
Bank mass failure
Macrochannel
Self-limiting threshold

ABSTRACT

A channel evolution model (CEM) represents stages of channel development in response to specific types of disturbance. In recent years, classic incised/disturbed CEMs have provided process-based understanding of channel adjustment and formed the cornerstone for river restoration and rehabilitation. While broadly applicable to alluvial systems in temperate and semi-arid regions, these models cannot be assumed to be universally applicable. Lockyer Creek in South East Queensland, Australia, has notable macrochannel morphology and is subject to high hydrological variability typical of many subtropical climates. The aim of this paper is to present a case study of channel adjustment and evolution in lower Lockyer Creek, to determine if existing CEMs adequately describe processes of channel adjustment and the associated trajectories of change typical of river systems in subtropical settings. Lockyer Creek has recently been subjected to a spate of flooding resulting in significant channel erosion. This offers an ideal opportunity to investigate the nature and rate of channel adjustment processes and place them in context of longer-term geomorphic adjustments in these systems. Specifically we address two questions. Firstly, do the classic incised/disturbed CEMs adequately represent the observed macrochannel adjustment? Secondly, if current CEMs are inadequate, what is the channel evolution model for these systems, of which lower Lockyer Creek is an example? Results show that these are non-incising systems where wet-flow bank mass failures (WBMFs) are the dominant process of channel adjustment. They occur within the channel bank top boundary resulting in no change to overall bank-top width. Furthermore, subsequent floods deposit sediment in the failure scars and failure headwalls generally do not retreat beyond channel bank-top. Channel adjustment has not followed the evolutionary stages for incised/disturbed channels and a new four stage macrochannel CEM is outlined for these subtropical systems. The proposed CEM illustrates a cyclical pattern of erosion by channel bank WBMF followed by re-aggradation, through deposition and oblique processes, contributing to bank rebuilding. This CEM provides sufficient information to determine the stage of macrochannel adjustment, enabling decisions to be made over whether intervention is required or will be successful.

1. Introduction

Natural rivers exhibit various channel forms based on their discharge and sediment loads which integrate the effects of climate, vegetation, soils, geology and basin physiography (Knighton, 1998). Change in any of these variables may, but not without exception, be expected to result in channel adjustment over time. As well as response to such allogenic factors, autogenic channel adjustment can occur due to internal adjustments such as meander migration leading to neck cut-offs, or levee aggradation leading to avulsion (Schumm et al., 1996). Evidence of past channels and their geometry are generally archived in adjacent floodplains and serve as reminders of such channel adjustment. Knowledge of these past adjustments or trajectories of change are important for predicting likely future trends and for setting realistic targets for river management that accommodate adjustments (Brierley and Fryirs, in press, 2005; Brierley et al., 2008), and move beyond application of steady-state equilibrium models derived from elsewhere that aim to produce 'stable channels'.

Phillips (2011) proposes that collectively the principles of gradient selection and threshold-mediated modulation can provide a thesis of why rivers have particular forms, or emergent properties, which may *mimic steady states*. Gradient selection implies that mass and energy fluxes in geomorphic systems occur along the steepest gradients and persist and grow. Here, the downslope flow of water is an example where concentrated pathways once initiated are preferred if external factors are maintained. Threshold-mediated modulation in geomorphic systems implies that there are upper and lower limits to system development governed by a process threshold. Exceeding a threshold limits the process and may switch it in the opposite (or different) direction (Phillips, 2011). For example, levee and floodplain aggradation may eventually limit the frequency of overbank deposition. The resulting

* Corresponding author.
E-mail address: c.thompson2@uq.edu.au (C.J. Thompson).

http://dx.doi.org/10.1016/j.catena.2015.12.012
0341-8162/

flood confinement to the channel and greater depth of flows may then switch process from overbank deposition to channel bed erosion. The switch to erosional processes may prevail until some resistant basal material is reached limiting further bed erosion, or local base level reduces energy gradient and switches the process back to bed deposition. This threshold modulated switching between process modes has also been used to explain divergent and convergent landform evolution and switches between divergence and convergence (Phillips, 2014). Divergent evolution results in spatial heterogeneity, an increase in statistical variance of an indicator variable and has multiple possible end states. In contrast, convergent evolution results in spatial homogeneity, a decrease in statistical variance of an indicator variable and a single end or stable state. Convergence and a single end or stable state is often preferred in river management where stable river channel geometries can be used as templates for design (e.g. Rosgen, 2007). Divergence has been viewed as problematic by river managers who have set in place programs to maintain stable states without understanding that threshold-mediated modulation can limit divergence and switch to convergence. Hence, the principles of gradient selection and threshold-mediated modulation may be used to understand the magnitude, duration and direction of geomorphic adjustment.

Channel geometry describes the three-dimensional form of a channel and four degrees of freedom have been proposed to represent the planes of adjustment of this geometry through sediment erosion and deposition on channel banks and beds (Knighton, 1998). These four degrees of freedom are: cross-sectional form, bed configuration, planimetric geometry and channel bed slope. Schumm et al. (1984) developed a five stage channel evolution model (CEM) to explain the complex channel response to disturbance which incorporates all four planes. Stage I represents the perceived stable or initial channel form (Fig. 1). Stage II represents the

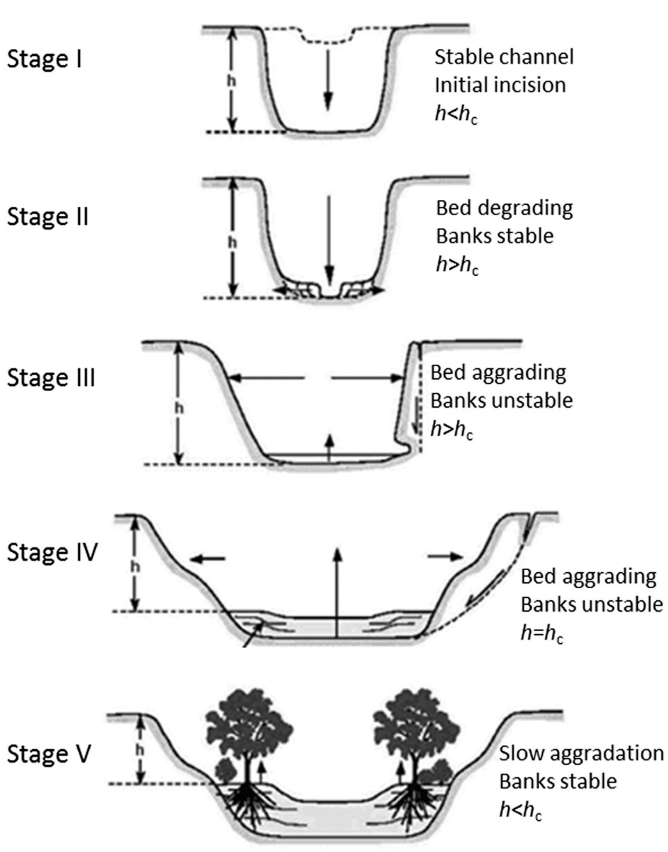

Fig. 1. Stages of classic channel evolution model of Schumm et al. (1984). *h* represents bank height and h_c is critical bank height.
Modified from http://www.austintexas.gov/faq/geomorphic-analysis.

initiation of channel bed degradation, whether direct and instantaneous due to channelization or indirect through alteration to water and sediment fluxes in a landscape. In Stage III degradation leads to exceedance of critical bank height, resulting in channel widening via bank mass failures. Stage IV sees a switch to bed aggradation and continued widening as the channel gradient decreases and knickpoints migrate upstream. Stage V marks the return to a quasi-equilibrium channel as bank slopes decrease, vegetation stabilizes the new inset floodplain and meander migration further reduces longitudinal slope. Simon (1989) describes a six stage CEM, slightly modified from Schumm et al. (1984), based around anthropogenic modification of West Tennessee channels. These CEM's have been developed and most commonly used to describe geomorphic adjustments that occur in fully alluvial rivers over timescales of 10^1–10^2 years in response to both natural and anthropogenic disturbances.

Embedded within both the Schumm et al. (1984) and Simon (1989) models, the cycle of bank erosion explains how bed and bank (in)stability occurs at various stages (Brierley and Fryirs, 2005; Pizzuto, 1984; Thorne, 1982; Thorne and Lewin, 1979; Thorne and Tovey, 1981). As such, both CEMs have gained widespread acceptance and use in temperate and semi-arid North America, albeit with minor variations in sequencing owing to the type and scale of disturbance and the regional setting (e.g. Cluer and Thorne, 2014; Hawley et al., 2012; Heitmuller, 2014). The model has been evaluated for similar settings in Europe (e.g. Bollati et al., 2014) and temperate southeast Australia (e.g. Page and Carden, 1998). The effect of reafforestation in Europe has resulted in differing response trajectories following the initial stage of channel incision (Liebault and Piegay, 2001; Rinaldi and Simon, 1998). Given the similarity and widespread use of these CEMS, they will be referred to hereon as the classic CEMs.

The most common range of physical processes that can occur in a river system are represented by these classic CEMS. This results in their widespread use in channel restoration programs to determine the current morphological trajectory of a disturbed channel and to guide selection of the appropriate channel engineering works to return the system back to one of "stability" (i.e. Stage I) (e.g. Bledsoe et al., 2002; Hawley et al., 2012; Watson et al., 2002). However, these classic CEMs assume that: (1) rivers are fully alluvial; (2) there is no local bedrock control inhibiting incision; (3) the bed and banks are unconstrained and able to adjust; and (4) the system state preceding the initial disturbance stage represents a stable or steady state equilibrium. Given that all rivers do not fulfil these assumptions, the widespread use of these classic CEM's for interpreting geomorphic processes and identifying causes of channel degradation, particularly in river restoration practice, has been called into question (Hawley et al., 2012; Phillips, 2009).

Recently, South East Queensland (SEQ) has experienced a spate of floods causing significant channel erosion. A detailed description of the geomorphic processes which occurred during these floods is provided in Croke et al. (2013a), Grove et al. (2013), Thompson and Croke (2013) and Thompson et al. (2015). As part of the analysis into the recent SEQ floods Grove et al. (2013) determined that a significant proportion of the erosion could be accounted for as a result of wet-flow bank mass failure (WBMF). The more traditional bank erosion processes of slab, rotational or cantilever failures were not observed. Here, WBMF were caused predominantly by piping and sapping processes. Exfiltration from saturated or near-saturated banks on the falling limb of the flood hydrograph was sufficient for sediment removal from the bank and no significant volumes of sediment was left resting on the failure floor (Grove et al., 2013). Following the floods, major efforts have been underway to retard this erosion and return these channels to pre-flood conditions across the SEQ region on the assumption that this will improve the resilience of catchments to future floods. The template for restoration in SEQ has often been based on the assumption that channel response will follow the classic CEMs, and that engineered bank toe protection will prevent the system from proceeding through the classic CEM Stages III–V (e.g. Cardno Entrix, 2014).

The aims of this paper are to firstly, consider the morphology, hydrological variability and erosion-deposition processes that occur within the main boundary of a macrochannel system prior to, and following flooding, and secondly determine whether the classic CEMs adequately represent these channel adjustments, and if not develop a revised CEM that adequately captures the dominant processes and stages of adjustment occurring in these systems. This process understanding is required to ensure that the causes of change are correctly identified and appropriate treatments emplaced that aim to build flood resilience.

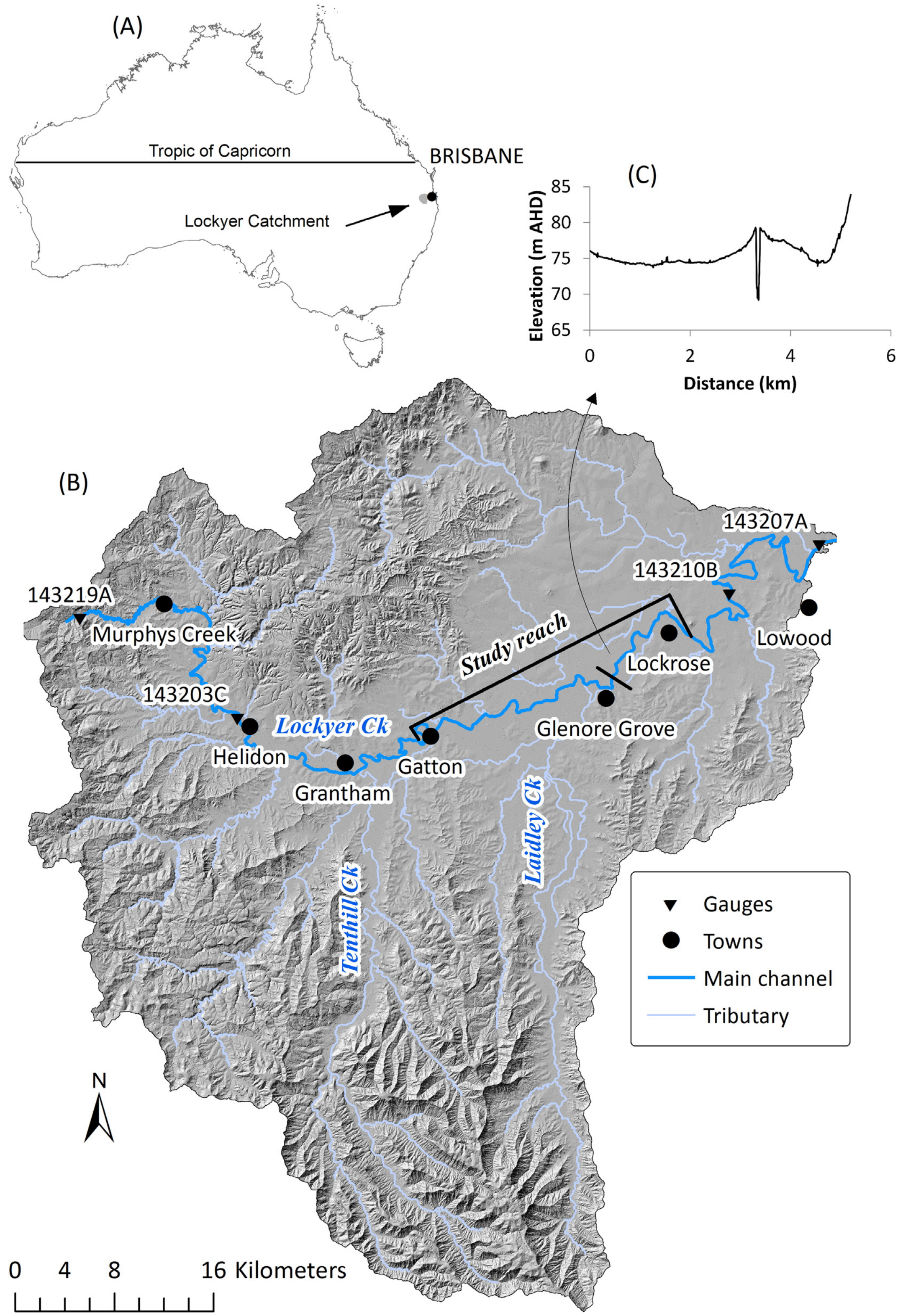

Fig. 2. (A) Study area is in the Brisbane catchment in eastern Australia below the Tropic of Capricorn. (B) Lockyer Creek subcatchment (~3000 km^2) with location of the study reach. (C) Representative cross section from study reach across location of WBMF sampled for grain size analysis which is illustrated in more detail in Fig. 3.

2. Study area

2.1. Catchment

The study was conducted on Lockyer Creek (~3000 km^2) a subcatchment of the Brisbane River in SEQ, Australia (Fig. 2). The headwaters drain the Great Dividing Range (~800 m Australian Height Datum (AHD)) delivering water and sediment to the wide floodplain which supports one of Australia's most productive horticultural regions with a Gross Region Product of $166 million in 2011/12 (LVRC, 2013). Discharge from Lockyer Creek forms part of the Brisbane City water supply, hence water quality is of major concern to water resource agencies.

The catchment geology comprises Main Range Volcanics (olivine basalt) on the divide. The headwaters have incised down to and flow across the Marburg subgroup (Jurassic sandstones, siltstones, and shale). Quaternary alluvium deposits commence near Helidon bounding the main channel down to the mid-Brisbane River confluence which encompasses the study reach (Fig. 2). The Quaternary alluvium overlies sandstone (Marburg subgroup) which displays large entrenched subsurface channel(s) (QDNRM, 2014).

The climate is subtropical with mean maximum monthly temperatures ranging between 21 and 29 °C. The total annual rainfall ranges between 900 and 1800 mm, with the majority falling during the warm summer season (October to February) (Bureau of Meteorology, BoM, 2012).

There have been major anthropogenic land-use changes in the Lockyer Valley. Indigenous communities in the Lockyer Valley used fire to clear trees and brush and promote grassland health prior to European settlement (Tew, 1979). European settlement commenced in the 1820s and at this time the landscape was described as having mixed forests with abundant grassland plains and pastures in close proximity to Lockyer Creek (Steele, 1972). Sheep grazing occurred in the early to mid-19th century. Widespread vegetation clearance from floodplains followed with the onset of cropping and dairy in the late 19th century. Development of irrigated farmland occurred through the early to mid-20th century. The late 20th century saw the expansion of crop farming at the expense of dairy farming on the fertile floodplains. Since European settlement, two-thirds of native vegetation has been cleared for agricultural purposes (Apan et al., 2002). The abundance of riparian vegetation adjacent to the main channel was highly variable through the 20th century but there is a noticeable increase in within-macrochannel vegetation density since the early 1970s. Most clearing of woody vegetation occurs on pastoral land (Apan et al., 2002), but hillslopes have remained forested throughout the 20th century. Small to medium (<8 m wall) weirs have been built along Lockyer Creek to manage the stream flow for agriculture and potable water supplies.

2.2. Lower Lockyer Creek

For the purpose of this study, lower Lockyer Creek is defined as the main channel from Tenthill Creek at Gatton, down to Lockrose which is also the downstream boundary of remote sensing time series data (Fig. 2). The study reach is 36 km long with a sand-bed and has a single thread planform that alternates between low sinuosity reaches and tight meandering bends which abut bedrock and other confining media (e.g. fine-grained cohesive floodplains). The mean bed slope of the reach is 0.00083 m m^{-1}. Bank height ranges from 9 to 19 m and bank top width varies between 80 to 190 m. Natural levees occur on both banks with approximately equal heights, which vary from 1 to 9 m along the reach (Thompson et al., 2014). Channel geometry of the lower Lockyer is variable, but is persistently large with bankfull discharge greater than a 10 year recurrence interval event (Croke et al., 2013b). The channel does not convey a single dominant discharge but is disposed to high hydrological variability. The channel form has been described as a macrochannel which is defined as a 'channel-in-channel' form where a smaller, low flow channel is inset within a larger channel, and separated from the margins of the macrochannel by geomorphic units such as benches, ledges, and various bar types (J.C. Croke et al., 2013). Soil bordering the channel and levee consists of dark clay loam to light clay with dark brown neutral to alkaline structured subsoil (Powell, 1987). Floodplain soils surrounding the levee are generally described as dark self-mulching, cracking medium to heavy clay (Powell, 1987).

2.3. Flow history and floods

The region is characterized by seasonally variable patterns of floods and droughts that have been linked to the interannual rainfall variations of the El Niño–Southern Oscillation (ENSO) and the Interdecadal Pacific Oscillation (IPO) (Kiem et al., 2003; Rustomji et al., 2009). Flash flood magnitude index (FFMI), calculated as the standard deviation of the logarithm of the annual maximum flood series, is a measure of flood variability with indices >0.6 indicating large flood variability (Baker, 1977; Erskine, 1993). FFMI for Lockyer Creek ranges from 0.66 to 1.08 which is representative of SEQ catchments indicating a propensity for alternating extremes (Rustomji et al., 2009).

The Helidon gauge has the longest flow record on Lockyer Creek, extending back to 1926. The 2011 flood is the largest recorded; however, other large floods in this record include four in the 1990s and five in the 1980s. The largest flood on record at Helidon prior to 2011 was 1974. The Brisbane River Record at the City Gauge which is 130 km downstream of the confluence with Lockyer Creek shows nine 'major' flood events preceding the 2011 floods, the majority of which occurred prior to 1900 and after European settlement. Six floods were of a higher magnitude than the 2011 floods, including those of 1841 and 1893 that were the largest on record prior to 1974 (Bureau of Meteorology, BoM, 2013; Van den Honert and McAneney, 2011).

The conditions for the largest flood were a strong La Niña event in the summer of 2010–11 which led to above average rainfall. This resulted in high soil moisture and elevated groundwater levels across the catchment. On 10 January 2011, the soils were already saturated when a number of massive storm cells converged and moved across the top of the catchment and intensified. Peak two-hour rainfall intensities over the headwaters had annual exceedance probabilities (AEPs) that ranged up to 1 in 1088 years based on radar data (Rogencamp and Barton, 2012). Highest measured rainfall intensity for one-hour duration was 94 mm h^{-1} recorded in Toowoomba on the catchment divide and west of the highest intensity observed from the radar data. The extreme rainfall resulted in flash flooding through the upper catchment, significant loss of life and significant geomorphic change (Thompson and Croke, 2013). Once flood waters reached the lower Lockyer, the transmission speed slowed and the flood hydrograph broadened due to the combination of overbank flow and lower tributary inflows (Croke et al., 2013b) (Table 1).

The summer of 2012–13 was dry in comparison to 2010–11 until late January 2013 when ex-tropical Cyclone Oswald delivered widespread flooding rains to eastern Queensland as it moved slowly south. Rainfall intensity was less than in 2011 for the Lockyer catchment with annual exceedance probabilities (AEP) generally between 1 and 2% (BoM, 2013). However, Laidley Creek (Fig. 2), a main tributary of the Lockyer set a new stage height record due to receiving up to 710 mm in 24 h and 944 mm over two days in its headwaters (Mt Castle Alert #540171). However, the lower Lockyer stage height was less than in 2011 while still exceeding bankfull capacity (Table 1).

3. Methods

3.1. DEMs and geomorphic change detection

The spatial and temporal scales of geomorphic change are drawn from LiDAR data and near-coincident high resolution aerial photography captured from three time periods: (T_1) October 2010; (T_2) February–March 2011, and (T_3) March–June 2013 which bookend the 2011 and 2013

Table 1
Flood characteristics.

Gauging station	Record length (year)	Catchment area (km^2)	2011				2013			
			Qp[a] (m^3 s^{-1})	Duration (h)	ARI[b]	Mode water depth at LiDAR capture (m)	Qp (m^3 s^{-1})	Duration (h)	ARI[b]	Mode water depth at LiDAR capture (m)
Spring Bluff (143219A)	34	18	361.5	2.5	55	1.84	40.7	35.5	6	1.8
Helidon (143203ABC)	87	357	3642	3	693	0.8	433	60	6	0.75
Riffle Range Road (143210AB)	49	2490	–	128	–	2.0	1238	112	10	1.2
O'Reilly's Weir (143207A)	65	2965	2976	312	23	8.0	2160	181	12	7.9

– indicates no data due to flood exceeding ratings curve limit at gauging station.
[a] Peak discharge (Qp) represents instantaneous discharge.
[b] Average Return Interval (ARI) is derived from Log Pearson type 3 distributions of annual maximum flood series inclusive of 2013 record.

floods. Each capture had different spatial extents but, overlapped to allow for 36 km of main channel to be analyzed. Stage heights were similar between 2011 and 2013 LiDAR capture time, but stage height was lower for 2010 capture (Table 1). The water extent at the 2011 stage of capture was used as a mask and removed from subsequent analysis. The T_1 LiDAR was acquired with a Leica ALS50-11 Airborne Laser Scanner producing an average point density of 2 points/m^2, and data were post-processed by AAM™. The T_2 LiDAR was acquired with a Riegl LMS-Q680 airborne laser scanner producing approximately 4 points/m^2 and post-processed by Terranean™. The T_3 LiDAR was acquired with a TopoSys Harrier 68i airborne laser scanner producing approximately 2.13 points/m^2 and post-processed by RPS Mapping.

LiDAR point clouds were generated for each survey flight line from the full waveform LiDAR signal and translated from the temporal/angular units to geographic coordinates by reference to the calculated flight trajectories. Residual errors were measured to provide an initial quality check of the LiDAR data. The overlapping LiDAR flight lines were leveled and combined, and then adjusted to ground control to produce a set of LAS files. No additional merging multidate LiDAR scenes were conducted.

Survey points from the LAS files were filtered to remove any visually obvious anomalies and blunders before deriving a triangular irregular network (TIN) using Delaunay triangulation for each LiDAR capture. A 1-m-resolution Digital Elevation Model (DEM) was subsequently used throughout the analyses reported here. The resultant pre- and post-flood DEMs were differenced by subtracting the elevations in each DEM on a cell-by-cell basis to produce DEMs of Difference (DoD). Error and uncertainty in the DEM surfaces were identified and quantified following methods described in Wheaton et al. (2010) and applied using the Geomorphic Change Detection (GCD) software (http://gcd.joewheaton.org/home). The three steps to account for uncertainty consisted of (i) quantifying the surface representation uncertainty in the individual DEM surfaces; (ii) propagating the identified uncertainties into the DoD; and (iii) assessing the significance of propagated uncertainty.

To quantify surface representation uncertainty in the individual DEM surfaces, a minimum level of detection (minLoD) was used to distinguish actual surface changes from inherent noise (Fuller et al., 2003). Survey control marks (SCMs) classified as good from a permanent survey control database (https://www.business.qld.gov.au/industry/titles-property-construction/surveying/permanent-survey-marks) were used as the point of truth to quantify the uncertainty in the individual digital elevation models using root-mean-square-error (RMSE). SCMs are monuments that provide a physical realization of one or more datums which are an official, fully defined spatial reference surface to which measurements may be defined and related. The SCMs adhere to the standard set by the Intergovernmental Committee on Surveying and Mapping (ICSM) (2014).

$$\mathrm{RMSE} = \sqrt{\frac{1}{n}\sum_{t=1}^{n}(x_{2,t}-x_{1,t})^2} \quad (1)$$

x_2 is the recorded height value for the survey control mark and x_1 is the height value extracted from the digital elevation model. The RMSE values were 0.0733 m (342), 0.0748 m (322), and 0.0628 m (342) for T_1, T_2 and T_3 respectively with the number of SCM in parentheses. The standard deviation of error (SDE) values were 0.0724 m, 0.0740 m and 0.0621 m for T_1, T_2 and T_3 respectively. The similarity between RMSE and SDE values indicate low systematic error. This was investigated further by comparing a post processed kinematic (PPK) survey, captured by a vehicle mounted differential GPS after the 2013 flood along sealed roads throughout the catchment which have not undergone any repair during the period of LiDAR data capture, to each DEM. Based on a subset of 3420 points adjacent to the study reach, elevation differences between PPK points and the 2010, 2011 and 2013 DEMs were 0.09 m ± 0.18, 0.01 m ± 0.16 and 0.01 m ± 0.11 respectively. The slightly larger difference for the 2010 DEM is assumed to represent the degree of road subsidence that may have occurred following the 2011 event owing to the nature of black cracking and self-mulching floodplain soils which required many kilometers of sealed road to be repaired. The 2011 and 2013 height differences are well below the minLoD and therefore no further corrections were applied.

Uncertainties were propagated into DoDs using the approach of Wheaton et al. (2010) by:

$$\delta u_{DoD} = \sqrt{(\delta z_{new})^2 + (\delta z_{old})^2} \quad (2)$$

where δu_{DoD} is the propagated error in the DoD assuming that error in each cell is random and independent, and δz_{new} and δz_{new} are the individual errors in the $\mathrm{DEM_{new}}$ and $\mathrm{DEM_{old}}$ respectively. The SDE values were used as estimates of δz, and the combined error was calculated as a uniform value for the entire DoD. While spatially variable error surfaces can provide improved DoD accuracy (i.e., geomorphic change estimates can be less conservative than if applying a uniform error surface; Wheaton et al., 2010), ground truthing of representative sites supported the propagated uncertainty derived from the uniform error surface which may be due to the low banks slopes of the macrochannels and the flat topped benches.

The significance of the uncertainty manifested in each DoD was approximated using probabilistic thresholding (Brasington et al., 2003; Lane et al., 2003). A critical threshold error was based on a critical Student's *t* value at 95% confidence interval. An error reduced DoD is then obtained by removing elevation changes with probability values less than the chosen threshold (Wheaton et al., 2010). Field site investigation and high resolution air photos provided good agreement with locations of erosion and deposition and relative depths derived from the error reduced DoD.

3.2. Derivation of geomorphic units

Mapping of key geomorphic units (inner channel, bench and macrochannel banks) was required to evaluate the CEM. The extent of macrochannel banks and channel benches were classified and mapped using terrain analysis, HEC-RAS hydraulic modelling and HEC-GeoRAS for interpolating model output across the DEM in ArcGIS. The method is described in detail in Croke et al. (2013a). In summary, hydraulic modelling was conducted to create three DEM subsets, (1) an inner (low flow) channel containing the channel bed, based on $Q_{2.33}$ discharge, (2) the macrochannel based on an iterative process to determine bankfull discharge and (3) floodplain. Removing subset (1) from subset (2) created a DEM of macrochannel banks and channel benches. These geomorphic units were differentiated by terrain slope (macrochannel banks > 14° ≥ bench). The classified macrochannel bank and bench DEM was converted to a polygon layer and used for segregating erosion and deposition into geomorphic units. To assess bank top width change, 300 cross sections spanning the macrochannel used for the hydraulic model were compared for each time period. Statistical difference was assessed using a paired *t*-test.

3.3. Bank mass failure mapping

BMFs were identified and mapped after the 2011 flood by Grove et al. (2013) using LiDAR data and high-resolution aerial photography. Thompson et al. (2013) mapped the extent of pre-existing BMF (present prior to the 2011 flood). Here, we have mapped the distribution of the 2013 flood-derived BMFs following the procedures described in Grove et al. (2013). In summary, a polygon layer was created of BMFs by tracing around the failure headwall on the aerial imagery, guided by the >35° slope layer derived from the LiDAR DEM to define the mass failures. As LiDAR does not penetrate water, a mask was placed over the inner channel and these data points were excluded from the analysis.

The variables measured and/or recorded for each mass failure determined whether the mass failure occurred on an 'intact' bank, or coincided with a previous failure. Failure length in the downstream direction, area and volumetric change which includes both erosion and sediment deposition, were also quantified.

Sediment samples were taken from around the sidewall and headwall of a BMF for grain size analysis. Sieving was used to differentiate grains > 20 μm, and a hydrometer for particles ≤ 20 μm. Sediment deposited during the 2013 flood in the base of a BMF and adjacent at mid-bank height were also sampled for grain size analysis.

3.4. Channel bed incision and vegetation coverage

Water in the channel prevented the use of LiDAR data for assessing channel bed change during the recent floods. Instead, the assessment of channel bed incision and channel slope was derived from historical photos of bridge piers, mapping of weirs, and Queensland Government bore log data, which records depth to bedrock across the floodplain. Anecdotal evidence from landholders was also utilized.

Change and/or recovery of riparian vegetation were assessed qualitatively from field site observation and time series comparison of air photos before and after the floods which were collected at a higher temporal frequency than LiDAR data.

4. Results

4.1. Evidence to assess the applicability of the classic CEM

The classic CEM of Schumm et al. (1984) and Simon (1989) are predicated on a critical bank height being reached following channel bed incision (Fig. 1). Generally, bed incision is the initial channel response to change in sediment supply/transport capacity relationships or channelization, which then leads to a critical bank height being exceeded followed by channel bank widening via various BMF processes. In the later stages of the classic CEMs, bed aggradation and channel migration reduce the energy gradient and bank height reduces below critical. Here we evaluate the extent to which processes presented in classic CEMs hold true for application in the Lockyer Creek system.

4.1.1. Bed degradation and long profile slope adjustment

Elevation of the channel bed and the slope of Lockyer Creek are predominantly controlled by the underlying sedimentary bedrock. The topography of the sedimentary basin, as derived from groundwater bore logs (QDNRM, 2014), shows single- and multi-channel trenches which the current channel lies above, or adjacent to (Fig. 3). The bore log records also indicate paleo gravel lags above the bedrock. When the Creek is above this bedrock trench, the bed is ~20 m above the basement (e.g., Fig. 3C), however; when the creek runs outside the bedrock trench, the channel bed lies on, or just above, bedrock (e.g., Fig. 3B) with bedrock straths often visible in the banks. These irregularly spaced bedrock intersections vertically constrain the channel and thereby prevent or limit the rate of bed incision. Bedrock is exposed in the channel near the catchment outlet at the junction of the Lockyer with the mid-Brisbane River which provides a base-level control on slope adjustment.

In addition to bedrock controls, anthropogenic structures including small weirs have an average spacing of approximately 8 km along the main channel and have provided an additional grade control function over the past ~50 years (Fig. 3). Anecdotal reports from landholders along lower Lockyer Creek suggest that only localized scour and fill has occurred. An evaluation of historical airphotos and photos of historical bridge piers also showed no evidence of bed degradation over the past ~100 years (Fryirs et al., 2015). Evidence would suggest that channel bed incision is not a significant channel adjustment process occurring along the Lower Lockyer channel.

4.1.2. Channel bank top width and bend migration

Analysis of historical air photographs shows no evidence of meander bend extension or migration, nor significant changes in channel width since European settlement (Fryirs et al., 2015). The DoDs show that these processes were also inactive during the most recent phase of floods. For the most recent floods, no significant change in the channel bank top width is evident based on repeat cross section surveys across the three time periods of LiDAR ($p < 0.05$, $N = 368$) which had mean and standard deviation of 95.4 m ± 16.6, 95.6 m ± 16.7 and 96 m ± 16.9 for 2010, 2011 and 2013 respectively. The lack of planform adjustment via channel migration due to lateral stability of the macrochannel eliminates long profile slope adjustment as a form of adjustment that would normally be expected in the final stages of the classic CEMs.

4.2. Processes of erosion and deposition in Lockyer Creek macrochannel

Instead of changes in channel width, the 2011 and 2013 floods caused large volumes of erosion and deposition within the boundary of the macrochannel (Fig. 4). Erosion resulted from the processes of fluvial entrainment by excess shear stress and WBMF (Table 2). The mean volume of sediment eroded by fluvial entrainment was similar across bench and macrochannel banks. In contrast, WBMF which occupied less than one quarter of the area, displaced 2.2 times the volume of sediment than that eroded by fluvial entrainment in the 2011 flood and 1.3 times the volume eroded in the 2013 flood.

The stream-length density of WBMFs increased from 4.9 km^{-1} prior to 2011 flood to 25.1 km^{-1} after the 2013 event (Table 2). The majority of WBMFs occurred in a portion of channel bank where there is no topographical evidence of an existing WBMF. Overlap or intersection between old (pre 2010) and new (2011–2013) WBMFs along the channel bank increased from 17 to 45% respectively. Where intersections occur between WBMFs from different time periods, they were dominated by end-to-end coalescence (e.g. Fig. 4A). A lesser number of intersections resulted from WBMFs occurring higher on the bank than pre-existing WBMF, but <1% of WBMF resulted in headward extension into the floodplain. In these few cases, the WBMFs were located where overland flow had been concentrated forming drainage lines back into the main channel. Hence, each successive flood that causes WBMFs is reducing the channel bank area (or length) available for future WBMF and the space limitation is thereby resulting in more overlap

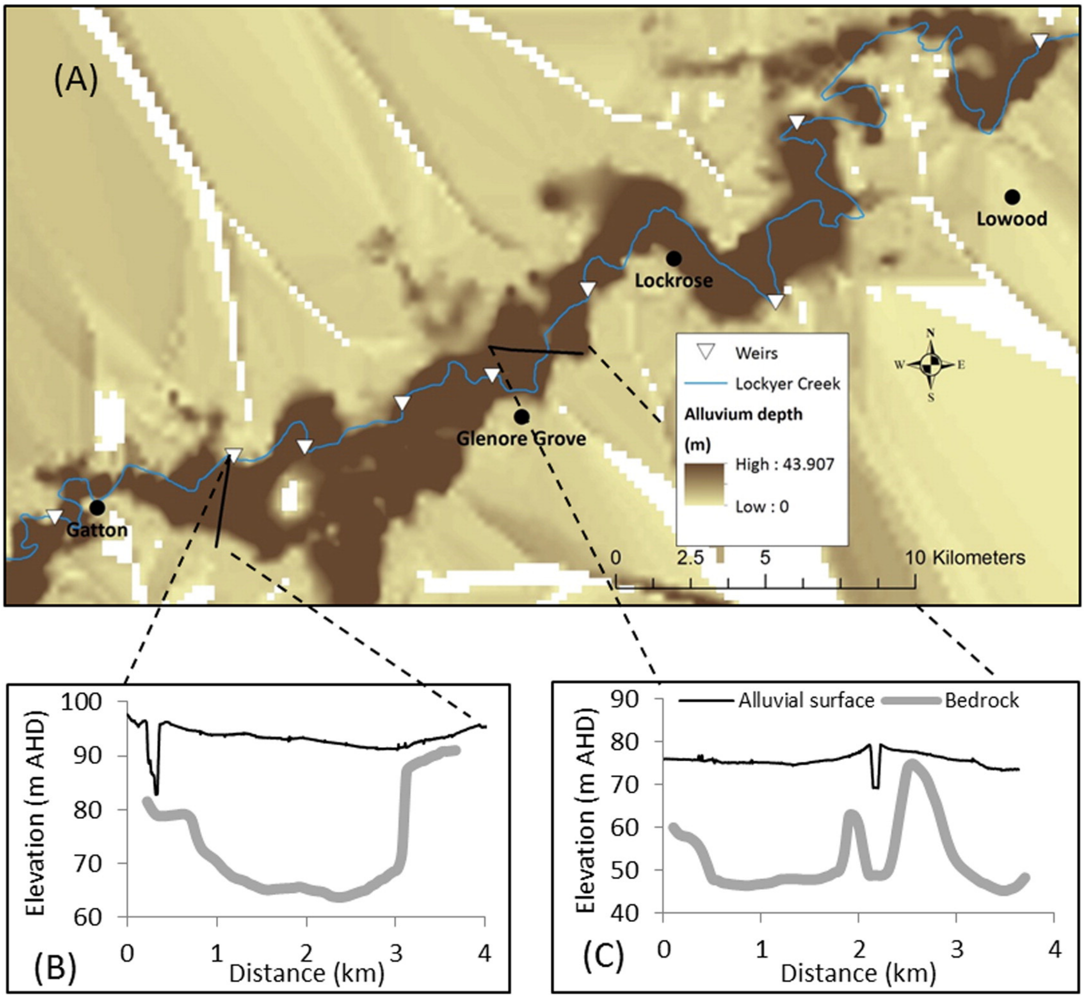

Fig. 3. (A) Current Lockyer Creek alignment relative to alluvial depth over bedrock and weirs. Inserted cross sections show (B) the current channel running outside the bedrock trench and (C) the channel running within the center of multiple bedrock trenches.

between WBMFs. After the 2013 flood, 50% of the length of the bank in the study area has been adjusted by WBMFs with some reaches exhibiting up to 70% of adjustment (Fig. 5).

Not all floods result in WBMFs and even the same flood can have a variable distribution of WBMF. For example, at around 25 km in Fig. 5 the densities of WBMF decrease. While this coincides with the confluence with Laidley Creek, there is no change in riparian vegetation, channel and floodplain morphology or bank height. However, differences in bank cross section profiles are evident between reaches which have incurred a high density of WBMF and reaches which have only sparse occurrence of WBMF with the former having convex profiles and the latter displaying linear profiles (Fig. 6).

A significant volume of the eroded sediment is re-deposited within the macrochannel on the banks, benches and within the erosional voids created by existing WBMFs. The average depth of deposition is 25–120% more in the WBMF scars than on banks and benches (Table 2). In terms of the void volume created by individual WBMFs, the percent in-filling of the 2011 WBMF voids by sediment deposited in the 2013 flood ranged from 0 to 100% with a median value of 21% (Fig. 7). The reason some WBMF scars had 0% in-filling is due to new WBMF intersecting or coalescing with an existing WBMF resulting in further erosion and removing the amount of sediment deposited. The initial phase of sediment deposition within the WBMF scars is comprised of coarse and fine sand which has a similar distribution to the deepest sediment (5.2 and 5.6 m) in the back wall of the failure scar of the channel bank (Fig. 8).

4.3. Vegetation change

Time series of airphotos and field photos spanning the 2011 and 2013 flood events illustrate vegetation change and rapid response time in the subtropical climate. Prior to the 2011 event the macrochannel contained a mix of grasses and trees (*Callistemon viminalis* lining the low flow channel and *Eucalyptus tereticornis* and *Eucalyptus tessellaris* scattered across the macrochannel bank) (Fig. 9A). The 2011 event removed much of this vegetation (Fig. 9B). Photos taken during fieldwork four months after the 2011 event reveal tall, dense grass indicating rapid growth and recovery (Fig. 9C). The vegetation covered the entire macrochannel (Fig. 9D) and invaded channel bars as flows decline (Fig. 9E). Five months after the 2013 event, grass, shrubs and young trees cover the entire channel obscuring geomorphic change (Fig. 9F).

5. Discussion

5.1. An alternative Channel Evolution Model for macrochannels

Our review of the available evidence would suggest that channel adjustment of lower Lockyer Creek has not followed the classic CEM stages as reported for temperate and semi-arid channels (e.g. Bollati et al., 2014; Cluer and Thorne, 2014; Hawley et al., 2012; Heitmuller, 2014; Rinaldi and Simon, 1998; Schumm et al., 1984; Simon, 1989; Simon

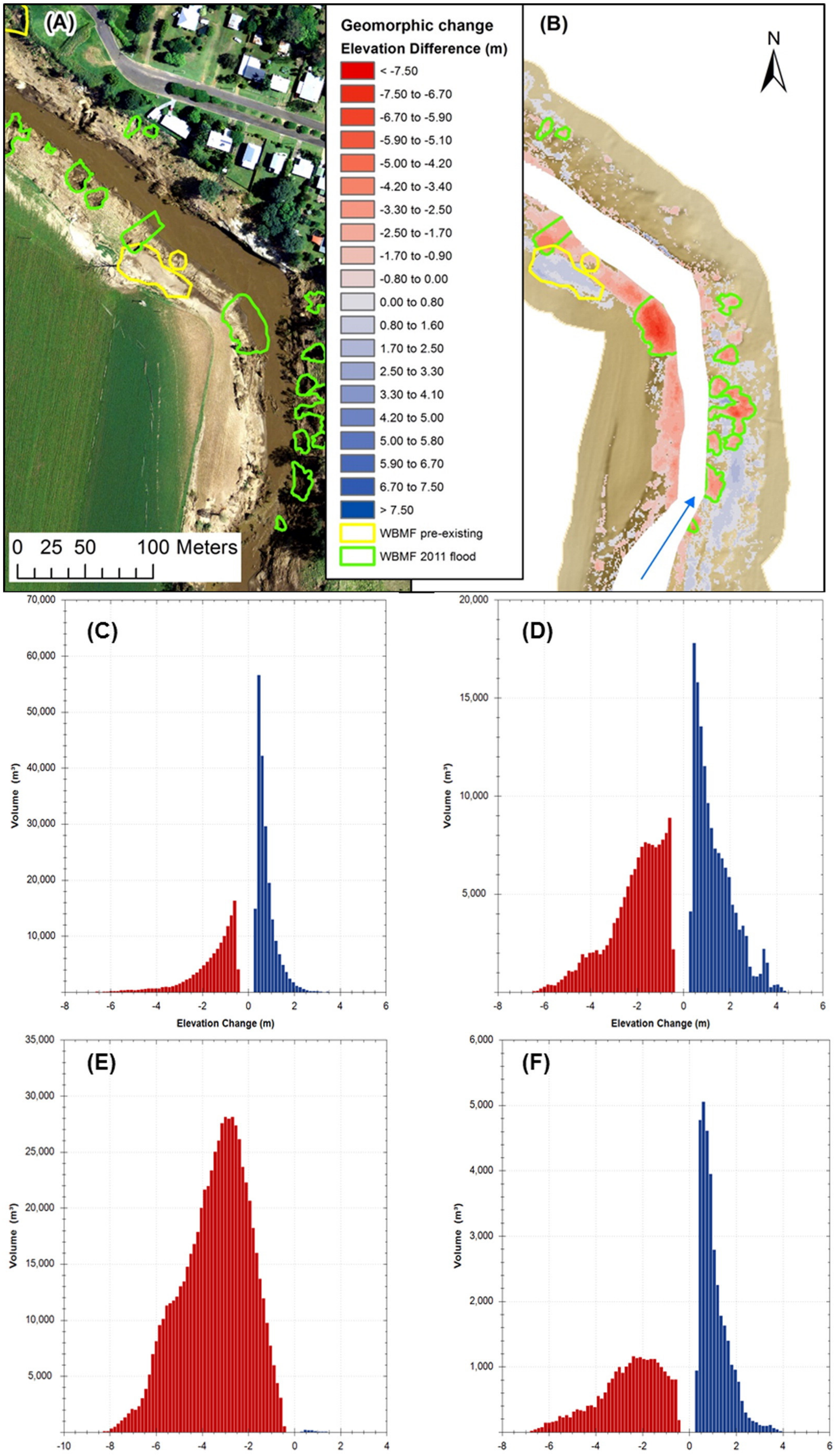
(A)
0 25 50 100 Meters
Geomorphic change
Elevation Difference (m)
< -7.50
-7.50 to -6.70
-6.70 to -5.90
-5.90 to -5.10
-5.00 to -4.20
-4.20 to -3.40
-3.30 to -2.50
-2.50 to -1.70
-1.70 to -0.90
-0.80 to 0.00
0.00 to 0.80
0.80 to 1.60
1.70 to 2.50
2.50 to 3.30
3.30 to 4.10
4.20 to 5.00
5.00 to 5.80
5.90 to 6.70
6.70 to 7.50
> 7.50
WBMF pre-existing
WBMF 2011 flood
(B)
N
(C)
(D)
(E)
(F)
Volume (m³)
Elevation Change (m)

and Hupp, 1986; Simon and Rinaldi, 2006). These classic CEMs assume that change is possible in all four degrees of freedom (Knighton, 1998): cross section, planform, slope and bed configuration. The results presented above for Lockyer Creek suggest that it is vertically constrained and laterally confined either by bedrock or resistant sediment (e.g. basal lags or fine-grained, cemented materials). Where macrochannels have been described elsewhere, evidence also confirms their lateral confinement by resistant fine grained sediments (Fryirs et al., 2015; Hoyle et al., 2008; Powell, 1987) and bedrock (e.g. Heitmuller et al., 2015). Thus, while the lower Lockyer macrochannel is predominantly an alluvial channel, it does not have four degrees of freedom to adjust. Channel planform and slope are inherited or controlled by exogenous factors.

A new four stage CEM for these hydrologically variable, subtropical, macrochannel systems is proposed (Fig. 10). This CEM depicts a macrochannel in which bank adjustments occur by WBMF followed by within macrochannel channel sediment deposition and aggradation aided by colonization and re-establishment of riparian vegetation. These processes are operating over timescales of 10^1–10^2 years in response to high magnitude–low frequency flood events.

5.1.1. Stage I: macrochannels and geomorphic convergence

Stage I of the model depicts a macrochannel with a conveyance capacity much greater than the mean annual flood (J.C. Croke et al., 2013). Macrochannel bankfull flow capacity has a median recurrence interval >10 years and a mode of 50 years for systems in subtropical Australia (Croke et al., submitted for publication) and accommodates a flow regime of high hydrological variability with no single dominant discharge.

The containment of most floods within the macrochannel promotes sediment deposition on banks and benches. Analysis of DoDs from the recent Lockyer floods showed significant volumes of sediment deposited within the macrochannel, with the 2013 event depositing more than the 2011 event. Net deposition was similar across macrochannel banks and benches. Deposited sediment was predominantly sandy sheets (Fig. 8) which aggraded vertically across the flat-topped benches and obliquely when draped across the bank slope. The different rates of aggradation between geomorphic units result in adjustments to bank profiles and the evolution of both convex and compound bank profiles comprising alternating layers of coarse and fine sediments. Dating of sediments from these banks and benches indicates ages of between 50 and 280 years old (J.C. Croke et al., 2013; Thompson et al., 2012) suggesting that decadal to centennial time scales of bank and bench aggradation occur to develop the convex and compound bank profiles that are a key process in the CEM. The product of changing bank profiles represents geomorphic convergence which could be represented as a decreasing mean and variance of channel width measured at mid-bank height if a sufficiently long time series of high resolution topographic data was available to quantify the gradual contraction in channel capacity.

5.1.2. Stage II: adjustment by wet-flow bank mass failure

WBMF was the primary process responsible for within macrochannel erosion, resulting in changes to the cross sectional area (Fig. 10). In general, mass failures are thought to occur via one of two main processes: (1) when critical bank height is exceeded after a phase of incision (Millar and Quick, 1998), or (2) when the basal support is eroded and the shear strength of the soil is exceeded by the weight of the overlying material (Thorne and Tovey, 1981). The latter may occur when the hydraulic conductivity (*Ks*) of the river sediment limits drainage so the water table cannot lower at the same rate as river stage (Dapporto et al., 2003).

Thompson et al. (2013) showed that there is no correlation between bank height and WBMF which contrasts with the findings reported in Simon (1989) who observed a critical bank height of around 8 m, above which slab and rotational failures occurred following channel incision. Thompson et al. (2013) also showed that there is no significant correlation between bank angle and WBMF, and no statistical difference in bank slope angles between those that failed and banks which did not. In the layered banks of the Lockyer Creek there were both sands with a high saturated conductivity and silty-clays with low saturated conductivity (e.g., Fig. 8). As the lateral support of the floodwater was removed on the receding limb, the exfiltration of bank and floodplain stored water kept the low conductivity layers saturated. This increased the weight of the bank material and also maintained a high pore water pressure that reduced friction. At the same time the sand layers produced piping flow that removed basal support. These conditions combined with the prolonged exfiltration caused the majority of the WBMFs along Lockyer Creek in 2011 and not the exceedance of a critical bank height (Grove et al., 2013). Many WBMFs have been mapped at mid-bank locations with an intact lower bank still present indicating that WBMFs are not dependent on fluvial entrainment of the bank toe which is a precursor for bank erosion and mass failure in the classic CEMs. Fluvial entrainment of the bank toe may still be a trigger in some of the failures, but it is not regarded as the critical factor in this system.

We propose that a self-limiting threshold exists based on the aggrading banks and the force of gravity acting on the load relative to the shear strength of a bank comprised of alternating fine and coarse strata. This sets-up, or primes the banks for WBMF (cf. Brewer and Lewin, 1998). Triggers for failure are (1) event magnitude and duration required to saturate the banks and (2) flood recession (draw down) which affects bank exfiltration from the high saturated conductivity bank layers. Banks not primed will not respond with WBMF when triggering processes occur (cf. Brewer and Lewin, 1998). This results in a differential response dependent on system proximity to thresholds (Brewer and Lewin, 1998; Richards, 1999; Schumm, 1979, 1973).

Stage II represents a process change from bank aggradation in Stage I to degradation as the WBMFs transform the convex bank profiles into concave profiles. Geomorphic divergence occurs as the frequency and density of WBMF increase during Stage II. This can be illustrated in planview with the increasing topographic heterogeneity (e.g. Fig. 4A) and an increase in mean and variance of the channel width measured at mid-bank height is expected as is characteristic of geomorphic divergence (Phillips, 2011). These processes occur on an event-by-event basis during high magnitude–low frequency flood events.

5.1.3. Stage III: in-filling of failure scars

A combination of WBMFs occurring while the stage was still relatively high, and the disintegration of the sediment into a fluid flow, results in rapid evacuation of the failed sediment by the receding floodwaters. Unlike other types of mass failures, there are no remaining loose blocks at the bank toe to act as basal protection. The limitation for further failure is instead provided by the increased cross sectional area and low flow width created by the WBMF scar which results in the formation of a low energy zone or slackwater zone (Fig. 11). The WBMF scar provides new accommodation space for sediment deposition. A similar process of erosional voids creating sediment accommodation space was described by Erskine (1996) based on bench destruction during a catastrophic flood and vertical accretion by subsequent flood events.

The process of channel capacity expansion by WBMF creating slackwater zones represents a self-limiting threshold to further bank erosion. The changed geometry that promotes sediment deposition represents a mode switch from bank degradation back to aggradation

Fig. 4. 2011 flood erosion and deposition: (A) from post-flood air photo from the top of the study reach, (B) the DoD of the same location illustrating locations of erosion and deposition, (C) histogram of volumetric change resulting from the 2011 flood for macrochannel banks, (D) benches, (E) new WBMF and (F) changes to pre-existing WBMF. The colored bars (red = erosion, blue = deposition) show significant geomorphic change based on 95% confidence interval. Note: variable y-axis scales.

Table 2
Volume of erosion and deposition, and bank mass failure characteristics for study reach. The volumetric changes in existing WBMFs has been calculated for each flood sequentially so that in 2013 the amount of erosion or deposition is presented for pre-existing BMFs, those failures that occurred in 2011, and those that were a consequence of the 2013 flooding.

Attribute	Pre-existing BMF	2011 BMF	2013 BMF	Macrochannel bank	Bench
Area of feature (m^2)	86,563	265,900	110,165	1,425,667	656,850
Flood 2011					
Erosion (m^3)	27,270 ± 3,912	662,404 ± 54,488	–	156,433 ± 46,357	156,148 ± 32,536
Deposition (m^3)	38,138 ± 10,899	1465 ± 521	–	294,834 ± 122,080	166,859 ± 47,628
Flood 2013					
Erosion (m^3)	15,577 ± 4,156	83,417 ± 19,478	255,619 ± 22,318	153,314 ± 56,231	127,887 ± 27,041
Deposition (m^3)	36,026 ± 9,755	103,299 ± 20,666	1319 ± 426	445,340 ± 139,008	174,268 ± 57,561
Number of WMBF	179	386	290	–	–
Density of WBMF (#/river km)	4.9	11.0	9.2	–	–
Overlap with existing BMF (%)	–	17	45	–	–

Dash represents no data.

(Fig. 10). In Lockyer Creek there have now been three events since the 2013 flood that has transitioned some reaches from Stage II into Stage III. These processes occur during intervening low–moderate flow conditions that may span years to decades.

5.1.4. Stage IV: geomorphic convergence and the influence of vegetation

Stage IV is represented by colonization and increasing density of vegetation within the sites of WBMF scars which increase hydraulic roughness, sediment trapping capacity and the tensile strength of sedimentary deposits as root networks establish (Erskine et al., 2009). Over time small–moderate floods continue depositing sediment layers of various caliber from sand to loam depending on flood magnitude and elevation of deposition surface, building benches (vertically) and reshaping the bank (obliquely). Similar processes and trajectories of adjustment have previously been described for post catastrophic flood recovery in hydrologically variable systems in eastern Australia (Erskine, 1996; Erskine and Livingstone, 1999; Webb et al., 2002). The bank profile evolves from concave at Stage II to convex moving through Stages III and IV as benches and banks aggrade and channel capacity decreases. This process differs from the bench evolution model of Erskine et al. (2009) which illustrated the evolution of point bars to benches with sediment deposition aided by vegetation colonization. In macrochannel systems linear bench tend to be more dominant than point benches, and it is the erosion void from the WBMF in the channel bank that are rebuilt, not just benches.

It is postulated that this adjustment pathway represents the principle of threshold-mediated modulation (the self-limiting thresholds) as described by Phillips (2014, 2011) which switches the channel bank evolution between modes of convergence (Stages III, IV & I) to one of divergence (Stage II), then back again.

5.2. Implications for existing understanding of channel adjustment

Current understanding in geomorphology suggests that channel dimensions are typically adjusted to accommodate a dominant discharge, often considered analogous to bankfull discharge (Ferro and Porto, 2012; Wolman and Miller, 1960) which on average is thought to have a recurrence interval of <5 years in many settings (e.g., Emmett and Wolman, 2001; Erskine and Keshavarzy, 1996; Petit and Pauquet, 1997; Woodyer, 1968). Although additional research indicates that identifying a single dominant or effective discharge is often problematic, it remains the most commonly accepted notion of channel adjustment. This study has described the stages of channel adjustment in a region of high hydrological variability where the existence of a macrochannel form indicates the occurrence of a range of infrequent high magnitude events and long periods of low flow. The bankfull discharge recurrence interval for a selection of gauging stations throughout the region of SEQ illustrate a mode of 50 years with a 5th–95th percentile range of 2–85 years (Croke et al., submitted for publication). The existence of WBMFs and their influence on channel geometry indicates that channel dimensions are not just strictly a function of available discharge. The occurrence of these features is highly dependent upon conditions of soil saturation and rapid changes in pore-water pressure as flood waters recede. Adjustments of cross sectional geometry through WBMFs within a residual boundary of the macrochannel is the dominant process in the proposed macrochannel CEM giving rise to a cyclical pattern of aggradation, then mode switching to degradation, before switching back again over timescales of 10^1–10^2 years. Given that the macrochannel in this system has not undergone significant geomorphic change since European settlement (Fryirs et al., 2015), and dating evidence suggests that the macrochannel was in place by at least the Late Holocene (Powell, 1987), it is suggested that the CEM presented here has been in operation for several hundreds of years or longer.

The lack of site specific associations between form and process has led to the conclusion that river systems are complex to degrees that can defy process explanations across a wide range of scales (Murray and Fonstad, 2008). In some studies, bank failures have been investigated within the concept of Self-Organized Criticality (SOC) which describes systems in which a set of local, but often different processes generates a singular global pattern represented by some critical threshold condition (Croke et al., 2014; Fonstad and Marcus, 2003). The

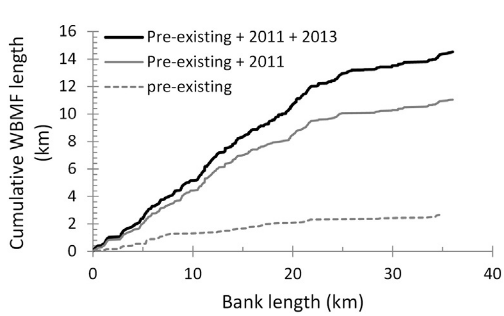

Fig. 5. Cumulative distribution of bank mass failures from three time periods; pre-2010, 2011 and 2013 along the study reach.

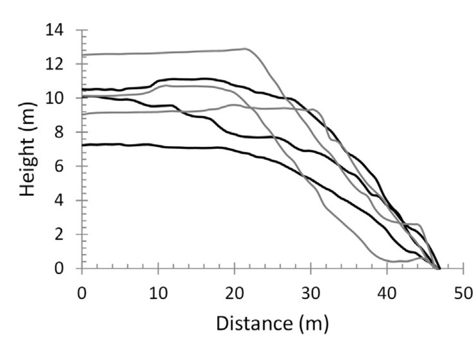

Fig. 6. Comparison of representative left bank cross section profiles from along high density WBMF reach illustrated by black lines (10–20 km in Fig. 5) and low a density WFMB reach illustrated by gray lines (25–33 km in Fig. 5). The representative bank profiles do not contain any WBMF.

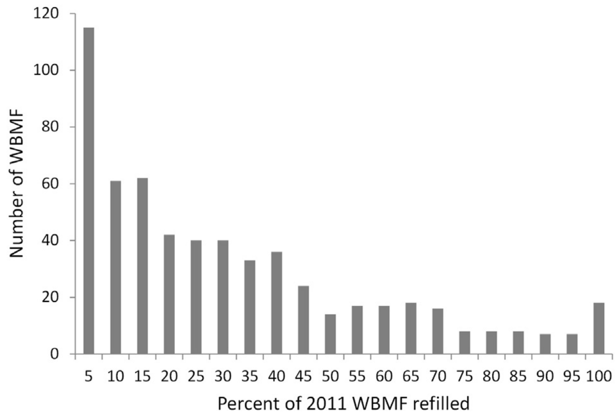

Fig. 7. Frequency distribution of percent refilling of 2011 WBMF by 2013 floods with sediment based on analysis of DoD for geomorphic change.

WBMFs in the Lockyer were found to display only weak and subjective evidence in support of SOC but available bank space was also identified as a self-limiting control on channel adjustment due to the tendency of WBMFs not to reoccur in the same location after successive floods. Overtime successive mass failures may interconnect, thus resetting overall macrochannel width and the available space for the re-aggradation of in-channel features. Results presented by Croke et al. (2014) confirm that our ability to 'predict' where such WBMFs occur is very low and as reported here in Stages III–IV of the CEM, these features will self-regulate over time through infilling and aggradation.

5.3. Implications for river management and flood resilience

The default for instream works in many river systems is stability rather than dynamic equilibrium. A current river management approach in subtropical Eastern Australia is to apply engineering solutions such as bank toe protection with engineered log jams and bank reshaping to return the channel to pre-flood form based on assumptions of channel change trajectories derived from the classic CEM (Cardno Entrix, 2014; Simon et al., 2012).

Proactive approaches to river management allow natural recovery processes to proceed, enhancing where possible the rate at which they occur (Brierley and Fryirs, 2009; Fryirs and Brierley, 2009; Rutherfurd et al., 2001). The macrochannel CEM provides the necessary understanding required to adequately determine the current stage of adjustment of a river reach (e.g. Fig. 12) and determine whether: 1) intervention is necessary, or whether the system should be left to adjust and recover naturally; and 2) if intervention is necessary whether it will be successful. The wrong intervention at the wrong stage of the CEM could induce secondary consequences that amplify process response and exacerbate threatening processes rather than ameliorate them (Kondolf, 2006). The proposed CEM, on-the-other-hand, indicates that within-macrochannel adjustment is self-modulating and it is possible for the system to naturally return to a previous state without the need for expensive engineering solutions. However, if accelerated

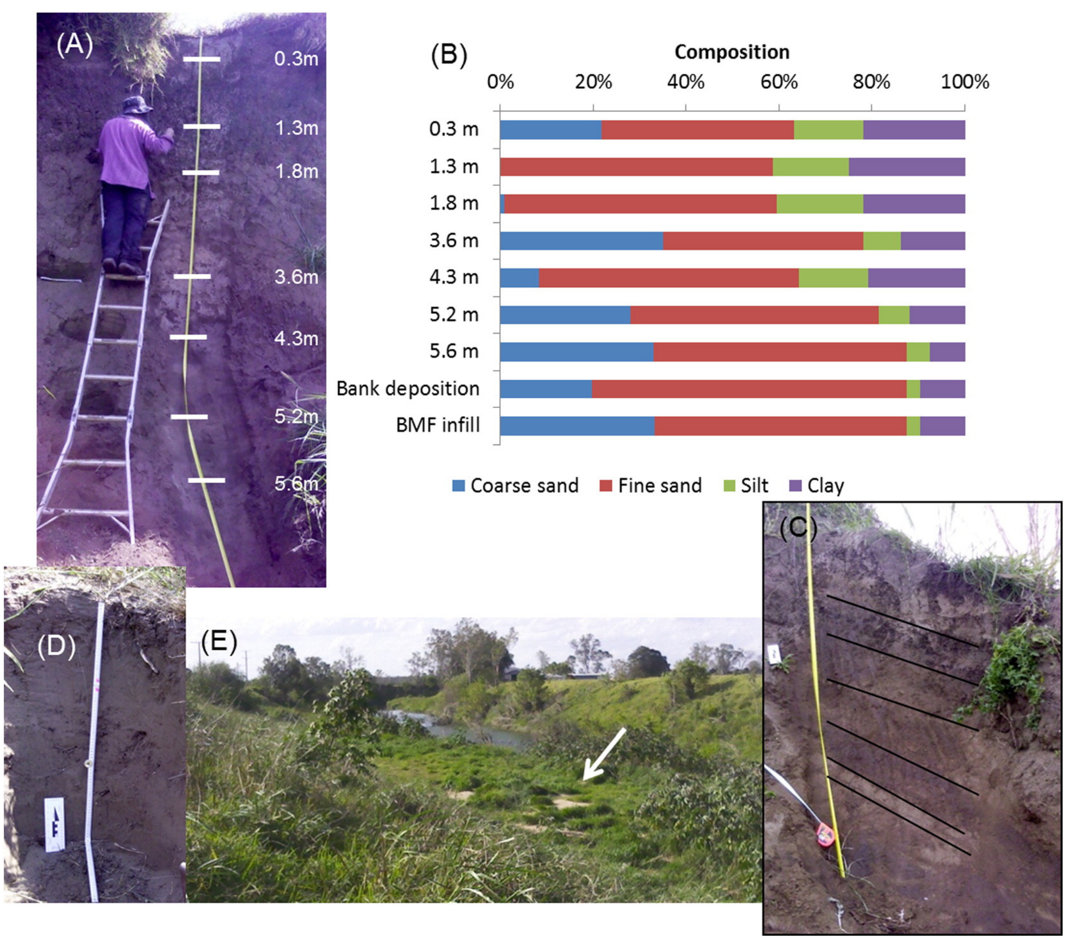

Fig. 8. (A,B) Sediment deposits and grain size distribution of samples collected from channel bank exposure of a BMF with (C) illustrating the diagonal or obliquely deposited sediment layer sloping down towards the channel. (D) shows a fine sand layer (75 cm thick) deposited across the macrochannel bank and (E) shows a sand sheet deposited across the top of a bench and now being colonized by grasses.

Fig. 9. Air photo time series spanning recent floods illustrating representative vegetation change on Lockyer Creek near Spencer St., Gatton.

sediment storage via bench and bank aggradation is a desired management outcome, then the proposed macrochannel CEM suggests that it may be most beneficial to intervene when a reach is at Stages III–IV once the system has switched from degradation back to aggradation. For example, this would encourage selected management actions that can accelerate the process of vegetation recovery to increase boundary

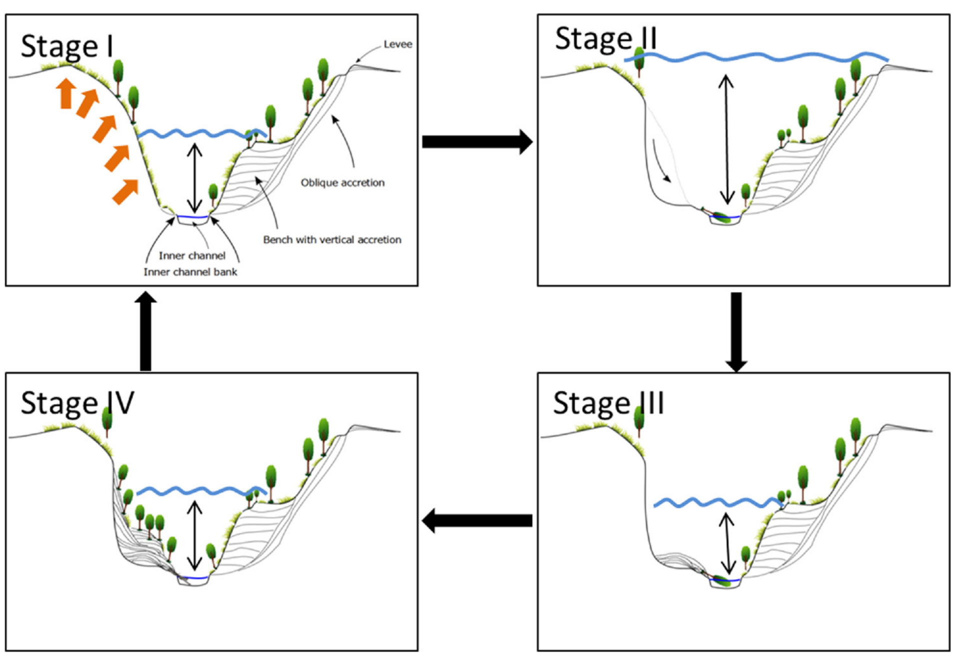

Fig. 10. A new CEM. Stage I represents the relatively large (macro)channel with bankfull capacity ≫ 10 year ARI. Broad up arrows indicate aggrading channel banks which have a convex or compound profile if benches are present. Double-headed arrows in channel represent flow regime over the annual to decadal scale. Stage II occurs once some upper limit of bank aggradation is achieved. Activation of BMFs requires long duration overbank events. No failed blocks remain due to type of failure and a concave bank profile results. The concave profile creates new sediment accommodation space and a low energy flow zone due to low flow width expansion. Stage III represents the start of deposition in the new accommodation space by subsequent floods. Stage IV represents continued sediment aggradation within the channel on banks and benches with increasing riparian vegetation enhancing sediment trapping and shear strength. The bank profile evolves from concave back towards compound and convex shape.

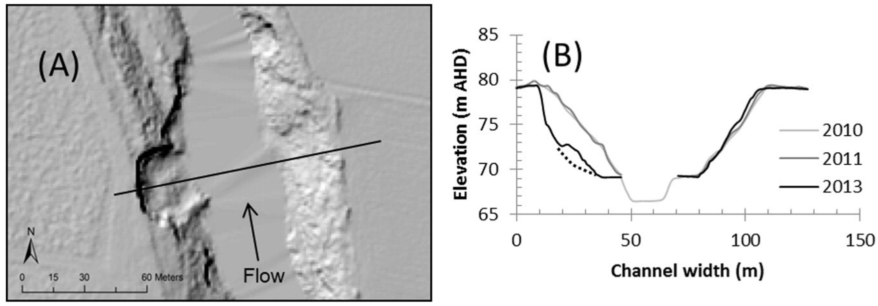

Fig. 11. Representative WBMF on Lockyer Creek illustrated in (A) planview with LiDAR DEM with Hillshade. The black line indicates the transect for (B) cross section profiles extrapolated from LiDAR data for time periods pre-2010, 2011 and 2013 showing change in channel geometry. Dotted line represents interpolation of the base of failure prior to sand deposition from subsequent small events.

resistance and sediment trapping efficiency (Bennett et al., 2002, 2008). There are a number of examples of pre-existing failure scars upon which native vegetation has established and maintained bench development while surrounding banks failed (82% of pre-existing BMF have not re-failed). Reaches that are currently at Stage II may be best left to adjust towards Stages III and IV before intervention.

6. Conclusions

The aim of this paper was to consider a CEM for macrochannel systems in a subtropical region using lower Lockyer Creek as a case study. This system has recently been subjected to a spate of flooding resulting in significant channel erosion. Results provided here suggest that the application of the classic CEM based around channel incision and widening is not appropriate for a macrochannel system. Macrochannels do not have four degrees of freedom to adjust even though they can be considered an alluvial channel. The macrochannel CEM depicts the process stages of evolution whereby bank adjustments occur via WBMF followed by within-channel sediment deposition and aggradation aided by colonization and re-establishment of riparian vegetation. It is postulated that degradation and aggradation processes are self-limiting resulting in mode switching and a cyclical pattern of adjustment.

It is envisaged that the new model is likely to be applicable to macrochannel systems across the subtropical climatic zone, which provide the conditions of high hydrological variability and rapid vegetation growth observed in the Lockyer. The existence of vertical accretion floodplain formation processes ensures that banks comprise alternating layers of high sandy units that have high saturated conductivity and silt- or clay loam units with low saturated conductivity, that prime the banks for WBMF. Constructing the new CEM required an understanding of the channel boundary conditions, dominate erosion processes, influence of vegetation in channel dynamics, and sedimentation patterns. This is similar to the model of Schumm et al. (1984) but supported by more spatially detailed data. Identifying different thresholds and processes of channel change, combined with an understanding of the processes of recovery during the relaxation period, should indicate criteria for validation of classic CEMs before they are applied.

The macrochannel CEM provides information required to determine the stage of channel adjustment and whether intervention is required or likely to be successful. Management actions can aid the process of sediment deposition and storage on within-channel benches and macrochannel banks in the later stages of the CEM through vegetation management. This work re-iterates the calls of many geomorphologists that any river rehabilitation efforts need to understand, and work with, natural processes characteristic of the given climatic, hydrologic and geomorphic setting (Brierley and Fryirs, 2009; Montgomery, 2008; Wohl, 2005). We believe the development of a revised CEM for this setting illustrates the need for and benefits of such an adaptive approach.

Acknowledgements

Funding for this research was from an ARC Linkage Project LP120200093, Industry partners DSITI, SEQwater and Lockyer Valley Regional Council. Thanks to Cate Dent for work on evaluating uncertainty in the 2013 LiDAR data and for Peter Todd providing PPK GPS data. CT would like to thank Jonathan Phillips for discussions on this work. We also thank Brian Sippel for access to sites on his property. Finally, we would like to thank the constructive comments from two anonymous reviewers which improved this paper. The authors declare no conflict of interest in this research.

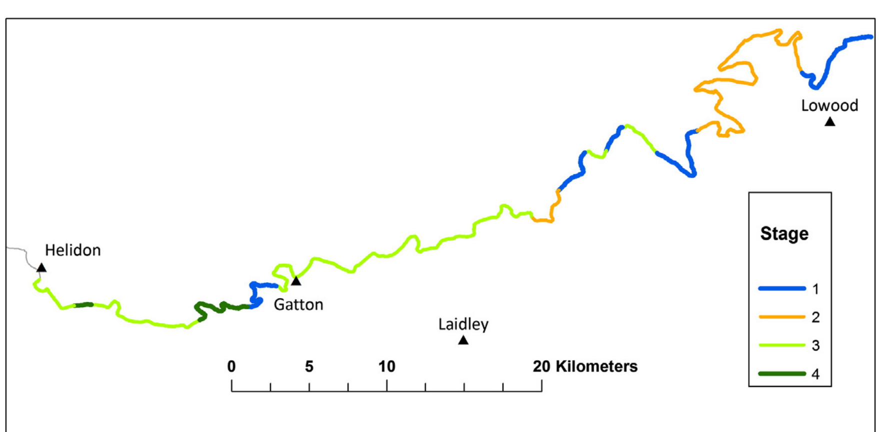

Fig. 12. Preliminary classification of macrochannel CEM Stages along Lockyer Creek. Grey line upstream of Helidon represents bedrock channel above the Quaternary alluvium.

References

Apan, A.A., Raine, S.R., Paterson, M.S., 2002. Mapping and analysis of changes in the riparian landscape structure of the Lockyer Valley catchment, Queensland, Australia. Landsc. Urban Plan. 59, 43–57.

Baker, V.R., 1977. Stream-channel response to floods, with examples from central Texas. Geol. Soc. Am. Bull. 88, 1057–1071.

Bennett, S.J., Pirim, T., Barkdoll, B.D., 2002. Using simulated emergent vegetation to alter stream flow direction within a straight experimental channel. Geomorphology 44, 115–126.

Bennett, S.J., Weiming, W., Alonso, C.V., Wang, S.S.Y., 2008. Modeling fluvial response to in-stream woody vegetation: implications for stream corridor restoration. Earth Surf. Process. Landf. 33, 890–909. http://dx.doi.org/10.1002/esp.1581.

Bledsoe, B.P., Watson, C.C., Biedenharn, D.S., 2002. Quantification of incised channel evolution and equilibrium. J. Am. Water Resour. Assoc. 38, 861–870.

Bollati, I.M., Pellegrini, L., Rinaldi, M., Duci, G., Pelfini, M., 2014. Reach-scale morphological adjustments and stages of channel evolution: the case of the Trebbia River (northern Italy). Geomorphology 221, 176–186.

Brasington, J., Langham, J., Rumsby, B., 2003. Methodological sensitivity of morphometric estimates of coarse fluvial sediment transport. Geomorphology 53, 299–316.

Brewer, P.A., Lewin, J., 1998. Planform cyclicity in an unstable reach: complex fluvial response to environmental change. Earth Surf. Process. Landf. 23, 989–1008.

Brierley, G.J., Fryirs, K.A., 2005. Geomorphology and river management: applications of the River Styles framework. Blackwell, Oxford, UK.

Brierley, G.J., Fryirs, K., 2009. Don't fight the site: geomorphic considerations in catchment-scale river rehabilitation planning. Environ. Manag. 43, 1201–1218.

Brierley, G.J., Fryirs, K.A., 2015. The use of evolutionary trajectories to guide 'moving targets' in the management of river futures. River Res. Applic. http://dx.doi.org/10.1002/rra.2930 (in press).

Brierley, G.J., Fryirs, K.A., Boulton, A., Cullum, C., 2008. Working with change: the importance of evolutionary perspectives in framing the trajectory of river adjustment. In: Brierley, G.J., Fryirs, K.A. (Eds.), River Futures: An Integrative Scientific Approach to River Repair. Island Press, Washington, D.C., USA, pp. 65–84.

Bureau of Meteorology (BoM), 2012. Annual Australian Climate Statement 2010/2011. Bureau of Meteorology (http://www.bom.gov.au/announcements/media_releases/climate/change/20120104.shtml).

Bureau of Meteorology (BoM), 2013. EXTC Oswald floods, January and February 2013. http://www.bom.gov.au/qld/flood/fld_reports/EXTC_Oswald.pdf.

Cardno Entrix, 2014. Channel and Bank Stability of Selected Reaches of the Burnett River System, Qld, Australia. http://www.bmrg.org.au.

Cluer, B., Thorne, C., 2014. A stream evolution model integrating habitat and ecosystem benefits. River Res. Appl. 30, 135–154.

Croke, J., Todd, P., Thompson, C., Watson, F., Denham, R., Khanal, G., 2013a. The use of multi temporal LiDAR to assess basin-scale erosion and deposition following the catastrophic January 2011 Lockyer flood, SE Queensland, Australia. Geomorphology 184, 111–126.

Croke, J., Reinfelds, I., Thompson, C., Roper, E., 2013b. Macrochannels and their significance for flood-risk minimisation: examples from southeast Queensland and New South Wales, Australia. Stoch. Environ. Res. Risk Assess. http://dx.doi.org/10.1007/s00477-013-0722-1.

Croke, J.C., Fryirs, K., Thompson, C.J., 2013c. Channel–floodplain connectivity during an extreme flood event: implications for sediment erosion, deposition, and delivery. Earth Surf. Process. Landf. 38, 1444–1456.

Croke, J., Denham, R., Thompson, C., Grove, J., 2014. Evidence of self-organized criticality in riverbank mass failures: a matter of perspective? Earth Surf. Process. Landf. 40, 953–964. http://dx.doi.org/10.1002/esp.3688.

Croke, J.C., Thompson, C.J., Daley, J., Fryirs, K., Lisenby, P., Lam, D., Dalla Pozza, R., Grove, J., Cohen, T., 2015. Defining the floodplain in hydrologically-variable settings: implications for flood magnitude-frequency analysis and interpretations of landscape resilience. Earth Surf. Process. Landf. (in review).

Dapporto, S., Rinaldi, M., Casagli, N., Vannocci, P., 2003. Mechanisms of river bank failure along the Arno River, central Italy. Earth Surf. Process. Landf. 28, 1303–1323.

Emmett, W.W., Wolman, M.G., 2001. Effective discharge and gravel-bed rivers. Earth Surf. Process. Landf. 26, 1369–1380. http://dx.doi.org/10.1002/esp.303.

Erskine, W., 1993. Erosion and deposition produced by a catastrophic flood on the Genoa River, Victoria. Aust. J. Soil Water Conserv. 6, 35–43.

Erskine, W.D., 1996. Response and recovery of a sand-bed stream to a catastrophic flood. Z. Geomorphol. 40, 359–383.

Erskine, W.D., Keshavarzy, A., 1996. Frequency of bankfull discharge on South and Eastern Creeks, NSW, Australia. 23rd Hydrology and Water Resources Symposium, Hobart, Australia 21–24 May 1996 vol. 2. Institute of Engineers, Australia, pp. 381–387 (Publication 96-05).

Erskine, W.D., Livingstone, E.A., 1999. In-channel benches: the role of floods in their formation and destruction on bedrock confined rivers. In: Millar, A.J., Gupta, A. (Eds.), Varieties of Fluvial Form. John Wiley and Sons, Chichester, UK, pp. 446–474.

Erskine, W., Chalmers, A., Keene, A., Cheetham, M., Bush, R., 2009. Role of a rheophyte in bench development on a sand-bed river in southeast Australia. Earth Surf. Process. Landf. 34, 941–953.

Ferro, V., Porto, P., 2012. Identifying a dominant discharge for natural rivers in southern Italy. Geomorphology 139-140, 313–321. http://dx.doi.org/10.1016/j.geomorph.2011.10.035.

Fonstad, M., Marcus, W.A., 2003. Self-organized criticality in riverbank systems. Ann. Assoc. Am. Geogr. 93, 281–296. http://dx.doi.org/10.1111/2F1467-8306.9302002.

Fryirs, K., Brierley, G.J., 2009. Naturalness and place in river rehabilitation. Ecol. Soc. 14, 20 (http://www.ecologyandsociety.org/vol14/iss1/art20/).

Fryirs, K., Lisenby, P., Croke, J., 2015. Morphological and historical resilience to catastrophic flooding: the case of Lockyer Creek, SE Queensland, Australia. Geomorphology 241, 55–71.

Fuller, I.C., Large, A.R.G., Charlton, M.E., Heritage, G.L., Milan, D.J., 2003. Reach-scale sediment transfers: an evaluation of two morphological budgeting approaches. Earth Surf. Process. Landf. 28, 889–903.

Grove, J.R., Croke, J.C., Thompson, C.J., 2013. Quantifying different riverbank erosion processes during an extreme flood event. Earth Surf. Process. Landf. 38, 1393–1406.

Hawley, R.J., Bledsoe, B.P., Stein, E.D., Haines, B.E., 2012. Channel evolution model of semiarid stream response to urban induced hydromodification. J. Am. Water Resour. Assoc. 48, 722–744http://dx.doi.org/10.1111/j.1752-1688.2012.00645.x.

Heitmuller, F.T., 2014. Channel adjustments to historical disturbances along the lower Brazos and Sabine Rivers, south-central USA. Geomorphology 204, 382–398.

Heitmuller, F.T., Hudson, P., Asquith, W.H., 2015. Lithologic and hydrologic controls of mixed alluvial–bedrock channels in flood-prone fluvial systems: bankfull and macrochannels in the Llano River watershed, central Texas, USA. Geomorphology 232, 1–19. http://dx.doi.org/10.1016/j.geomorph.2014.12.033.

Hoyle, J., Brooks, A., Brierley, G.J., Fryirs, K., Lander, J., 2008. Spatial variability in the timing, nature and extent of channel response to typical human disturbance along the upper Hunter River, New South Wales, Australia. Earth Surf. Process. Landf. 33, 868–889.

Intergovernmental Committee on Surveying and Mapping (ICSM), 2014). Standard for the Australian Survey Control Network — Special Publication 1 Version 2.1. Intergovernmental Committee on Surveying and Mapping, Canberra, Australia.

Kiem, A.S., Franks, S.W., Kuczera, G., 2003. Multi-decadal variability of flood risk. Geophys. Res. Lett. 30, 1035.

Knighton, D., 1998. Fluvial Forms and Processes: A New Perspective. Taylor & Francis.

Kondolf, G.M., 2006. River restoration and meanders. Ecol. Soc. 11 (2), 42 (http://www.ecologyandsociety.org/vol11/iss2/art42/).

Lane, S.N., Westaway, R.M., Hicks, D.M., 2003. Estimation of erosion and deposition volumes in a large, gravel-bed, braided river using synoptic remote sensing. Earth Surf. Process. Landf. 28, 249–271.

Liebault, F., Piegay, H., 2001. Assessment of channel changes due to long-term bedload supply decrease, Roubion, France. Geomorphology 36, 167–186.

Lockyer Valley Regional Council (LVRC), 2013. Economic Brief. Lockyer Valley Regional Council, January 2013.

Millar, R.J., Quick, M.C., 1998. Stable width and depth of gravel-bed rivers with cohesive banks. J. Hydraul. Eng. 124, 1005–1013.

Montgomery, D., 2008. Dreams of natural streams. Science 319, 291–292.

Murray, B., Fonstad, M.A., 2008. Preface: complexity (and simplicity) in landscapes. Geomorphology 91, 173–177. http://dx.doi.org/10.1016/j.geomorph.2007.07.011.

Page, K.J., Carden, Y.R., 1998. Channel adjustment following the crossing of a threshold: Tarcutta Creek, Southeastern Australia. Aust. Geogr. Stud. 36, 289–311.

Petit, F., Pauquet, A., 1997. Bankfull discharge recurrence interval in gravel-bed rivers. Earth Surf. Process. Landf. 22, 685–693.

Phillips, J.D., 2009. Changes, perturbations, and responses in geomorphic systems. Prog. Phys. Geogr. 33, 17–30.

Phillips, J.D., 2011. Emergence and pseudo-equilibrium in geomorphology. Geomorphology 132, 319–326.

Phillips, J.D., 2014. Thresholds, mode switching, and emergent equilibrium in geomorphic systems. Earth Surf. Process. Landf. 39, 71–79.

Pizzuto, J.E., 1984. Bank erodibility on shallow sandbed streams. Earth Surf. Process. Landf. 9, 113–124.

Powell, B., 1987. Nature, Distribution and Origin of Soils on an Alluvial Landscape in the Lockyer Valley, South-east Queensland Master of Rural Science Thesis University of New England.

Queensland Department of Natural Resources and Mines (QDNRM), 2014M. Groundwater Database — Queensland. http://dds.information.qld.gov.au/dds.

Richards, K.S., 1999. The magnitude-frequency concept in fluvial geomorphology: a component of degenerating research programme? Z. Geomorphol. Suppl. 115, 1–18.

Rinaldi, M., Simon, A., 1998. Bed-level adjustments of the Arno River, central Italy. Geomorphology 22, 57–71.

Rogencamp, G., Barton, J., 2012. The Lockyer Creek flood of January 2011: what happened and how should we manage hazard for rare floods. 52nd Annual Floodplain Management Association Conference (http://www.floodplainconference.com/papers2012.php).

Rosgen, D.L., 2007. River Stability Field Guide. Wildland Hydrology, Fort Collins, CO.

Rustomji, P., Bennett, N., Chiew, F., 2009. Flood variability east of Australia's Great Dividing Range. J. Hydrol. 374, 196–208.

Rutherfurd, I., Sheldon, F., Brierley, G., Kenyon, C., 2001. Third Australian Stream Management Conference Proceedings: The Value of Healthy Rivers. CRC for Catchment Hydrology, Melbourne.

Schumm, S.A., 1973. Geomorphic thresholds and complex response of drainage systems. In: Morisawa, M. (Ed.), Fluvial Geomorphology. University of New York, Binghamton, pp. 301–310.

Schumm, S.A., 1979. Geomorphic thresholds: the concept and its applications. Trans. Inst. Br. Geogr. 4, 485–515.

Schumm, S.A., Harvey, M.D., Watson, C.C., 1984. Incised Channels, Morphology. Dynamics and Control, Water Resources, Littleton, Colorado (200 pp.).

Schumm, S.A., Erskine, W.D., Tilleard, J.W., 1996. Morphology, hydrology, and evolution of the anastomosing Ovens and King Rivers, Victoria, Australia. Geol. Soc. Am. Bull. 108, 1513.

Simon, A., 1989. A model of channel response in disturbed alluvial channels. Earth Surf. Process. Landf. 14, 11–26.

Simon, A., Hupp, C.R., 1986. Channel evolution in modified Tennessee channels. Proceedings, Fourth Federal Interagency Sedimentation Conference, Las Vegas, March 24–27, 1986 vol. 2 (5–71–5–82).
Simon, A., Rinaldi, M., 2006. Disturbance, stream incision, and channel evolution: the roles of excess transport capacity and boundary materials in controlling channel response. Geomorphology 79, 361–383.
Simon, A., Brooks, A., Bankhead, N., 2012. Effectiveness of engineered log jams in reducing streambank erosion to the Great Barrier Reef: an example from the O'Connell River, Queensland, Australia. In: Grove, J.R., Rutherfurd, I.D. (Eds.), Proceedings of the 6th Australian Stream Management Conference, Managing for Extremes. River Basin Management Society, Canberra, Australia, pp. 252–257.
Steele, J.G., 1972. The Explorers of the Morton Bay District 1770–1830. Dai Nippon Printing Co. (International) Ltd., Hong Kong.
Tew, A.M., 1979. History of the Gatton Shire in the Lockyer Valley Gatton Shire Council.
Thompson, C.J., Croke, J.C., 2013. Geomorphic effects, flood power, and channel competence of a catastrophic flood in confined and unconfined reaches of the upper Lockyer Valley, southeast Queensland, Australia. Geomorphology 197, 156–169.
Thompson, C.J., Croke, J.C., Pietsch, T., 2012. The geomorphic impact of the January 2011 flood on Murphys Creek, southeast Queensland. In: Grove, J., Rutherfurd, I. (Eds.), Proceedings of the 6th Australian Stream Management Conference — Managing for Extremes, Canberra, 2012.
Thompson, C.J., Croke, J.C., Grove, J.R., Khanal, G., 2013. Spatio-temporal changes in river bank mass failures in the Lockyer Valley, Queensland, Australia. Geomorphology 191, 129–141.
Thompson, C., Croke, J., Dent, C., 2014. Potential impacts of levee construction in the Lockyer Valley. In: Vietz, G., Rutherfurd, I.D., Hughes, R. (Eds.), Proceedings of the 7th Australian Stream Management Conference, Townsville, Queensland, pp. 109–115.
Thompson, C., Fryirs, K., Croke, J., 2015. The disconnected sediment conveyor belt: patterns of longitudinal and lateral erosion and deposition during a catastrophic flood in the Lockyer Valley, southeast Queensland, Australia. River Res. Appl. http://dx.doi.org/10.1002/rra.2897.
Thorne, C.R., 1982. Processes and mechanisms of river bank erosion. In: Hey, R.D., Bathurst, J.C., Thorne, C.R. (Eds.), Gravel-bed Rivers. Wiley, Chichester, pp. 227–259.
Thorne, C.R., Lewin, J., 1979. Bank processes, bed material movement and planform development in a meandering river. In: Rhodes, D.D., Williams, G.P. (Eds.), Adjustments of the Fluvial System. Kendall/Hunt, Debuque, Iowa, pp. 117–137.
Thorne, C.R., Tovey, N.K., 1981. Stability of composite river banks. Earth Surf. Process. Landf. 6, 469–484.
Van den Honert, R.C., McAneney, K.J., 2011. The 2011 Brisbane floods: causes, impacts and implications. Water 3, 1149–1173.
Watson, C.C., Biedenharn, D.S., Bledsoe, B.P., 2002. Use of incised channel evolution models in understanding rehabilitation alternatives. J. Am. Water Resour. Assoc. 38, 151–160.
Webb, A.A., Erskine, W.D., Dragovich, D., 2002. Flood-driven formation and destruction of a forested flood plain and in-channel benches on a bedrock confined stream: Wheeny Creek, southeast Australia. In: Dyer, F.J., Thoms, M.C., Olley, J.M. (Eds.), The Structure, Function and Management Implications of Fluvial Sedimentary Systems. IAHS Publication no.276, pp. 203–210.
Wheaton, J.M., Brasington, J., Darby, S.E., Sear, D.A., 2010. Accounting for uncertainty in DEMs from repeat topographic surveys: improved sediment budgets. Earth Surf. Process. Landf. 35, 136–156.
Wohl, E., 2005. Compromised rivers: understanding historical human impacts on rivers in the context of restoration. Ecol. Soc. 10, 2 (http://www.ecologyandsociety.org/vol10/iss2/art2/).
Wolman, M.G., Miller, J.P., 1960. Magnitude and frequency of forces in geomorphic processes. J. Geol. 68, 54–74.
Woodyer, K.D., 1968. Bankfull frequency in rivers. J. Hydrol. 6, 114–142.